Bone histology of *Protoceratops andrewsi* from the Late Cretaceous of Mongolia and its biological implications

ŁUCJA FOSTOWICZ-FRELIK and JUSTYNA SŁOWIAK

Fostowicz-Frelik, Ł. and Słowiak, J. 2018. Bone histology of *Protoceratops andrewsi* from the Late Cretaceous of Mongolia and its biological implications. *Acta Palaeontologica Polonica* 63 (3): 503–517.

Protoceratops andrewsi is one of the best known and abundant ornithischian dinosaurs from the Djadokhta Formation (Late Cretaceous, Mongolia) and a subject of many morphological studies. Here we present the first study of its bone tissue (from the long bones, frill, and rib), describing microstructure, extent of remodeling, and growth tempo changes in ontogeny. Several specimens representing juvenile, subadult, and adult age stages have been studied. In general, paleohistology of *Protoceratops* is quite uniform throughout ontogeny, showing basic fibrolamellar bone complex with prevalence of woven-fibered bone and scarce remodeling. In adults the parallel-fibered bone matrix forms distinct although irregular zonation in the cortex until dominating it. The bone displays noteworthy abundance of fossilized fibers (including Sharpey's fibers), which apparently strengthen the tissue and enhance its elasticity. Growth tempo increased in the studied femora of *Protoceratops* at the subadult stage, which suggests changes in bone proportions (i.e., elongation of the hind limbs) in a similar manner as it was observed in a more basal *Psittacosaurus*.

Key words: Dinosauria, Ornithischia, Ceratopsia, paleohistology, ontogeny, growth tempo, Cretaceous, Mongolia.

Łucja Fostowicz-Frelik [lfost@twarda.pan.pl], Institute of Paleobiology, Polish Academy of Sciences, ul. Twarda 51/55, 00-818 Warsaw, Poland; and Key Laboratory of Vertebrate Evolution and Human Origins, Institute of Vertebrate Paleontology and Paleoanthropology, Chinese Academy of Sciences, Beijing 100044, People's Republic of China.
Justyna Słowiak [justyna.slowiak@twarda.pan.pl], Institute of Paleobiology, Polish Academy of Sciences, ul. Twarda 51/55, 00-818 Warsaw, Poland.

Received 23 January 2018, accepted 7 June 2018, available online 28 June 2018.

Introduction

Protoceratops andrewsi Granger and Gregory, 1923, a representative of basal neoceratopsians, was one of the most common dinosaurs in the Djadokhta Formation (Late Cretaceous) of the Gobi Desert, Mongolia (Granger and Gregory 1923; Brown and Schlaikjer 1940; Dodson 1976; Fastovsky et al. 2011; Hone et al. 2014). It was a relatively small herbivorous dinosaur living and nesting gregariously (You and Dodson 2004) in the hot semi-desert environs (Osmólska 1980; Jerzykiewicz et al. 1993; Fastovsky et al. 1997). Numerous, including complete, skeletons of these animals are known from Bayn Dzak (including "Shabarakh Usu" of Brown and Schlaikjer 1940), Toogreek (Jerzykiewicz and Russell 1991), and Tugrikin Shireh (= Tögrögiin Shiree; Fastovsky et al. 1997) localities in Mongolia. The abundance of fairly complete and well preserved specimens allowed multidirectional studies on skeletal morphology, mostly descriptive or concerning the functional aspects (Brown and Schlaikjer 1940; Tereshchenko 1994, 1996; see also Senter 2007; Maidment and Barrett 2014 for a broader taxonomical setting), behavior (Farlow and Dodson 1975; Hone et al. 2014, 2016; Fastovsky et al. 2011), ontogeny and development (Handa et al. 2012; Hone et al. 2014; Erickson et al. 2017), and intra-specific variability (Maiorino et al. 2015) of this dinosaur. Nevertheless, despite this plethora of morphological studies, the bone microstructure of *Protoceratops* has not been studied in depth, although some preliminary paleohistological observations on this species were presented by Makovicky et al. (2007). As to paleohistological studies, Ceratopsia in general were not extensively researched. The best known ceratopsian genus as regards the bone microstructure is probably *Psittacosaurus*. Studies by Erickson and Tumanova (2000) and Zhao et al. (2013) concerned the growth dynamics of *Psittacosaurus mongoliensis* and *P. lujiatunensis*, respectively, as inferred from the long bones microstructure. Additionally, Zhou et al. (2010) investigated the histology of the ossified epaxial tendons of *Psittacosaurus*. Horner and Lamm (2011) presented the first study of ontogenetic development of the parietal frill in a crown ceratopsid (*Triceratops*). Ours is the

first, albeit preliminary, survey of the bone microstructure of the basal neoceratopsian *Protoceratops andrewsi*. We sampled the long bones, a rib, and parietal frill of this dinosaur in order to investigate the ontogenetic changes of the bone microstructure and their implications for the biology of *Protoceratops*.

Institutional abbreviations.—ZPAL, Institute of Paleobiology, Polish Academy of Sciences, Warsaw, Poland.

Other abbreviations.—EFS, External Fundamental System; LAG, Line of Arrested Growth.

Material and methods

We studied the microstructure of the skeletal elements of *Protoceratops andrewsi* (Fig. 1) in two juvenile, three subadult, and four adult specimens (listed in Table 1). All specimens are housed at ZPAL.

For the purpose of this study we divided our sample according to their body size into juveniles (class I; approximately less than 30% of the femur length observed in the largest adult specimen), subadults (class II; between 30% and 70% of an adult size), and adults (class III). In determining the ontogenetic age of an animal we followed works concerning specifically *Protoceratops*, namely Handa et al. (2012) if the skull was associated with the skeleton (in the case of ZPAL MgD-II/3 and ZPAL MgD-II/35), and Hone et al. (2014, 2016) for the remaining specimens. We determine juveniles as specimens without any signs of maturity as per Hone et al. (2014) and subadults as representing a mixture of juvenile and adult features (e.g., ZPAL MgD-II/3, ZPAL MgD-II/35), after Hone et al. (2014, 2016).

The microanatomical terminology follows Padian and Lamm (2013). Specifically, we define a growth cycle observed in the bone section as the zone between well-defined marks of arrested or slowed growth (LAG or annulus, respectively).

Table 1. *Protoceratops* material used in this study.

Collection number	Locality	Ontogenetic status	Bone element
ZPAL MgD-II/3a–d	Bayn Dzak	subadult	parietal frill (a), rib (b), humerus (c), femur (d)
ZPAL MgD-II/8	Bayn Dzak	adult	ulna
ZPAL MgD-II/11a–c	Bayn Dzak	adult	femur (a), fibula (b), tibia (c)
ZPAL MgD-II/15	Bayn Dzak	subadult	humerus
ZPAL MgD-II/16a, b	Bayn Dzak	adult	humerus (a), femur (b)
ZPAL MgD-II/33	Bayn Dzak	adult	parietal frill
ZPAL MgD-II/35a–c	Toogreek	subadult	humerus (a), femur (b), tibia (c)
ZPAL MgD-II/407	Bayn Dzak	juvenile (ca. 16% of adult size)	femur
ZPAL MgD-II/408	Bayn Dzak	juvenile (ca. 30% of adult size)	tibia

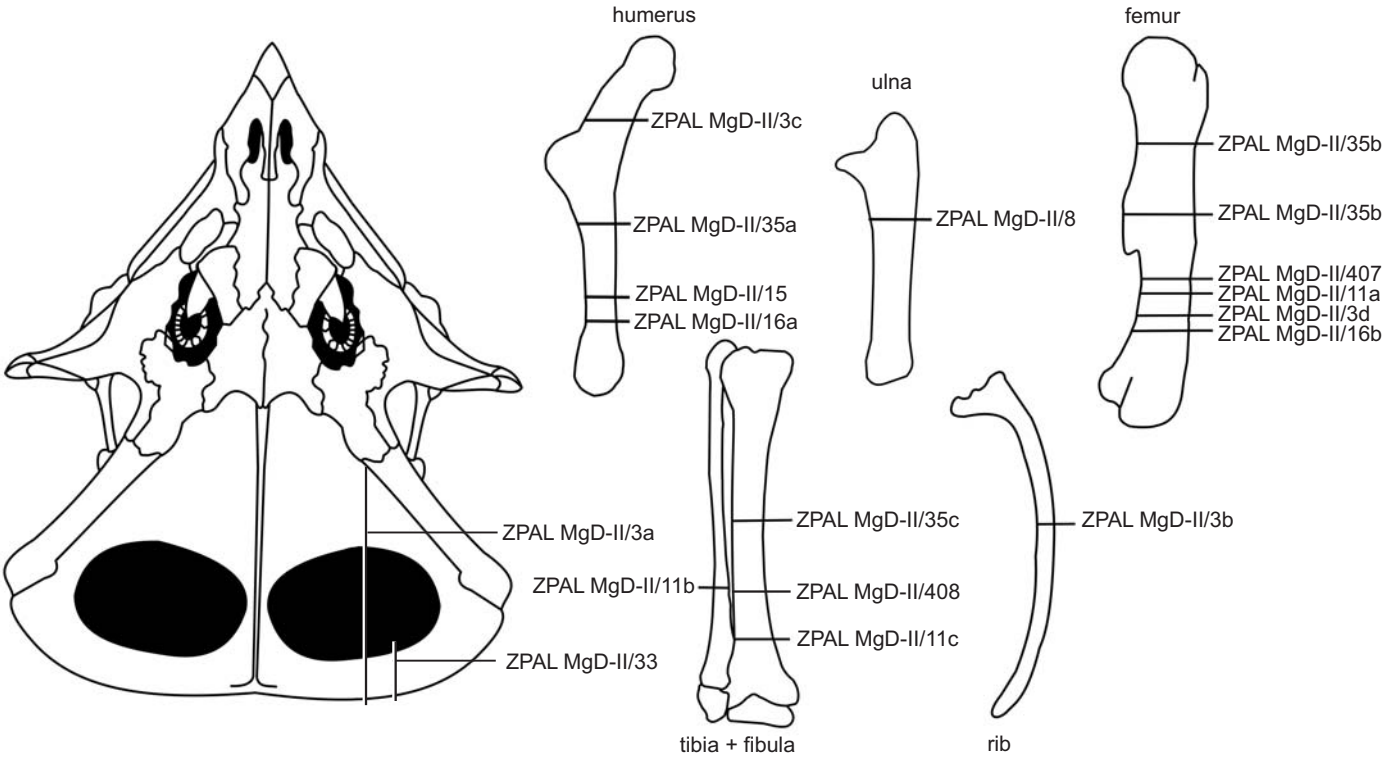

Fig. 1. Schematic drawing of the studied bones of *Protoceratops andrewsi* Granger and Gregory, 1923 showing the thin-section locations. Catalog numbers designate the studied individuals.

The best sampled individual (the long bones, frill, and rib) is an articulated, almost complete subadult skeleton ZPAL MgD-II/3 (Niedźwiedzki et al. 2012: fig. 1). For details of other sampled specimens see Table 1. We identified taxonomically all the specimens as belonging to *Protoceratops* on the basis of their morphology and association with the cranial material of that dinosaur, where applicable.

We sectioned the long-bones in the mid-shaft in complete bones, or as close as possible in damaged specimens. The bone samples were embedded in epoxy resin, then polished with silica powder following standard procedures (see e.g., Chinsamy-Turan 2005; Padian and Lamm 2013). The bone microstructure was studied in thin section using a Nikon Eclipse 80i transmitted light microscope fitted with a DS-5Mc cooled camera head under normal and polarized light, and under UV for imaging organic material. Additionally, large-scale thin sections were studied using a Nikon Eclipse LV100 POL polarizing microscope with a DS-Fi1 camera in transmitted normal and polarized light (also with a quartz wedge). The partial images were stitched with the help of NIS-Elements microscope imaging software (Nikon Instruments).

Results

General remarks on bone microstructure.—The long bone tissue of *Protoceratops andrewsi* shows a considerable prevalence of woven-fibered bone type, especially in the smallest studied specimens, where the lamellar component of a typical fibro-lamellar complex is poorly developed (Fig. 2A). In the perimedullar region the tissue porosity increases and a remodeling starts, initially with single secondary osteons (Fig. 2B), then with formation of the coarse cancellous bone, displaying endosteally originated lamellar bone tissue. The main difference between the age classes lies in the increase of the content of the parallel-fibered bone matrix in the outer cortex in larger specimens (Fig. $2A_1$, B_2), which signals a decreasing tempo of growth. The extent of remodeling is relatively low even in mature individuals, but it is much greater in the adult fibula and ulna than in the juvenile tibiae, where it is almost non-existing.

At the cellular level, the bone tissue shows a great abundance of osteocyte lacunae (Fig. 3A, B), especially well exposed in the studied tibiae (age class I and II), where they are visible in the woven-fibered bone matrix as well as within the osteon lamellae (Figs. $2B_1$, 3A). The osteocyte lacunae in the smallest studied specimen tend to be roundish to oval. In a larger but not fully grown tibia the lacunae are more condensed in the bone matrix surrounding the osteons, where they are more flattened (Fig. 3B). A darker mineral filling of the lacunae in some regions of the samples frequently exposes multiple branching canaliculi (Fig. 3B).

The bone tissue contains abundant fossilized fibers. A large portion of these fibers can be classified as Sharpey's fibers sensu stricto, as per Hall (2005). These are also the fibers most frequently observed in the fossilized bone (see Chinsamy-Turan 2005). Sharpey's fibers strengthen the internal cohesion of the bone tissue at the periosteum-cortex line in regions that are especially exposed to physical stress, such as at the points of muscle or ligament attachments. Thus, Sharpey's fibers according to Hall (2005) are defined mostly by their function and location, not by any specific microstructure. Hall (2005) mentions also other collagen fibers present in the bone tissue showing a similar radial orientation as Sharpey's fibers, but they are not associated with the areas of increased mechanical stress. Such the fibers, apart from controlling mineral deposition, further strengthen the bone. In the bone tissue of *Protoceratops*, particularly in the studied parietal frill, tibiae, and fibula, the fibers are especially well-preserved and permeate the entire bone (Figs. 3C, D, $4A_1$, C_1, 5A, B_3) . The fibers in the long bones are arranged mostly centripetally (Fig. $3C_1$), and they were so abundant that during mechanical preparation (polishing) they were released from the surrounding mineral bone content and accumulated on the surface (see Fig. 3D) in large quantities.

Frill.—The tissue of the frill has been studied in two specimens, one subadult (ZPAL MgD-II/3) and one fully grown individual (ZPAL MgD-II/33). The bone tissue forming the frill is highly porous woven-fibered bone matrix (Figs. 4, 5). The tissue is spongy and displays multiple elongated anteroposteriorly radially-oriented vacuities (especially in the smaller specimen). These cavities are well visible in the tangential section of the distal margin of the frill (Fig. 4B). The vacuities become less elongated and more irregular in the older specimen as well as towards the center of the frill, forming minute sinuses, divided by shorter and more irregularly oriented bone trabeculae. In the smaller specimen (ZPAL MgD-II/3) long parasagittally oriented canals dominate (Fig. $4A_1$, B, C), whereas in the larger specimen the entire frill tissue is pierced by numerous small in diameter and mostly irregular in shape vacuities (Fig. 5).

The bone tissue of the frill abounds with fibers. In the smaller specimen they are oriented mostly chaotically in the matrix, occasionally forming transversally directed bundles (Fig. 4A, B_2). In the larger specimen they tend to form a net of dense meshed fiber bundles, arranged around the small vacuities (Fig. $5B_2$, B_3).

The sagittal section of the distal rim of the frill in ZPAL MgD-II/3 shows the condensation of the fibers close to the dorsal and ventral external surfaces. The fibers are parallel to each other and positioned at an acute angle (ca. 45°) to the outer surface of the frill (Fig. 4A). In the larger specimen the outer layer is much thinner and most of the frill is highly porous filled with irregular trabeculae (Fig. 5). The surface of the frill is wavy, bearing small indentations of nascent erosion lacunae (Figs. $4B_1$, 5C).

The sagittal section of the frill plate sampled at the centre of the frill in the smaller specimen, shows a less vascularized and more compacted tissue (Fig. 4C). Observed vacuities (arranged mostly radially) are strongly compressed

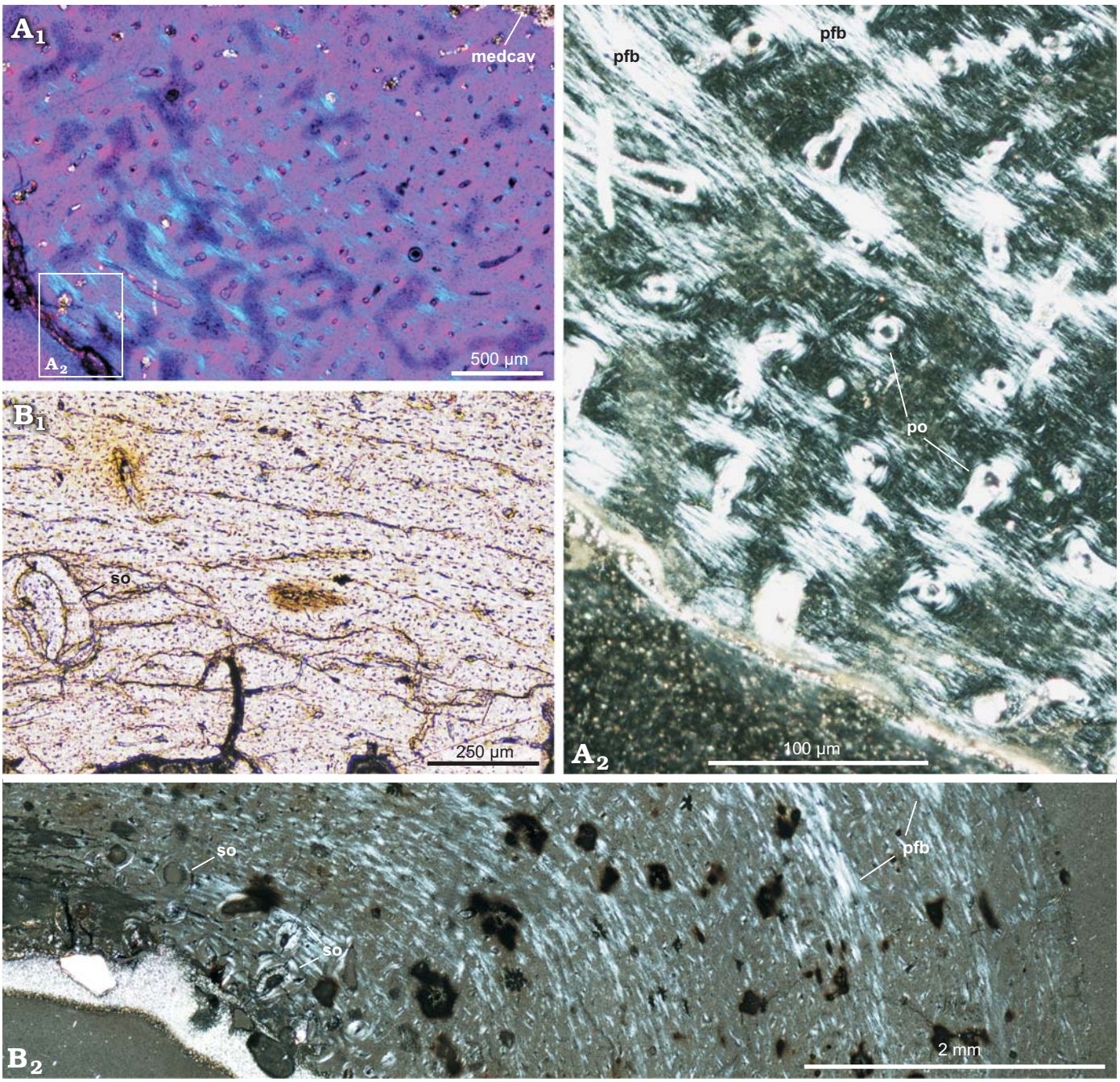

Fig. 2. Long bones microstructure of *Protoceratops andrewsi* Granger and Gregory, 1923, Bayn Dzak, Mongolia, Late Cretaceous. **A**. The shaft of the juvenile femur (ZPAL MgD-II/407) formed by a woven-fibered bone tissue; A_2, detail of A_1. **B**. The shaft of the subadult tibia (ZPAL MgD-II/35c) showing scarce erosion lacunae in the perimedullar region; B_1, detail of B_2. A_1, B_2, polarized light; A_2, polarized light (quartz wedge); B_1, normal light. Abbreviations: medcav, medullar cavity; pfb, parallel-fibered bone; po, primary osteons; so, secondary osteons (scarce).

dorsoventrally; the bone tissue is a primary woven-fibered bone but lacks primary osteons. The arrangement of bone fibers changes throughout the section (from dorsal to ventral direction) showing a discrete lamination. The dorsal part (ca. one-third of the bone thickness) shows two-to-three poorly differentiated layers consisting of fibers positioned at an acute angle to the outer bone surface (Fig. $4C_1$). The most internal part of the section displays horizontally oriented fibers, whereas the ventral part of the frill plate contains fibers showing some inclination towards the ventral bone surface. However, this inclination is weaker than that observed towards the dorsal surface, and the fibers are neither as condensed, nor well-organized in layers, as in the dorsal portion of the frill.

In the bone tissue of the smaller specimen there is no sign of remodeling or secondary bone tissue in all studied sections. In the larger specimen the vacuities (especially in the innermost part) are larger; thus, the bone erosion was more advanced, but secondary bone tissue is extremely scarce, restricted to the thin lining of erosion lacunae.

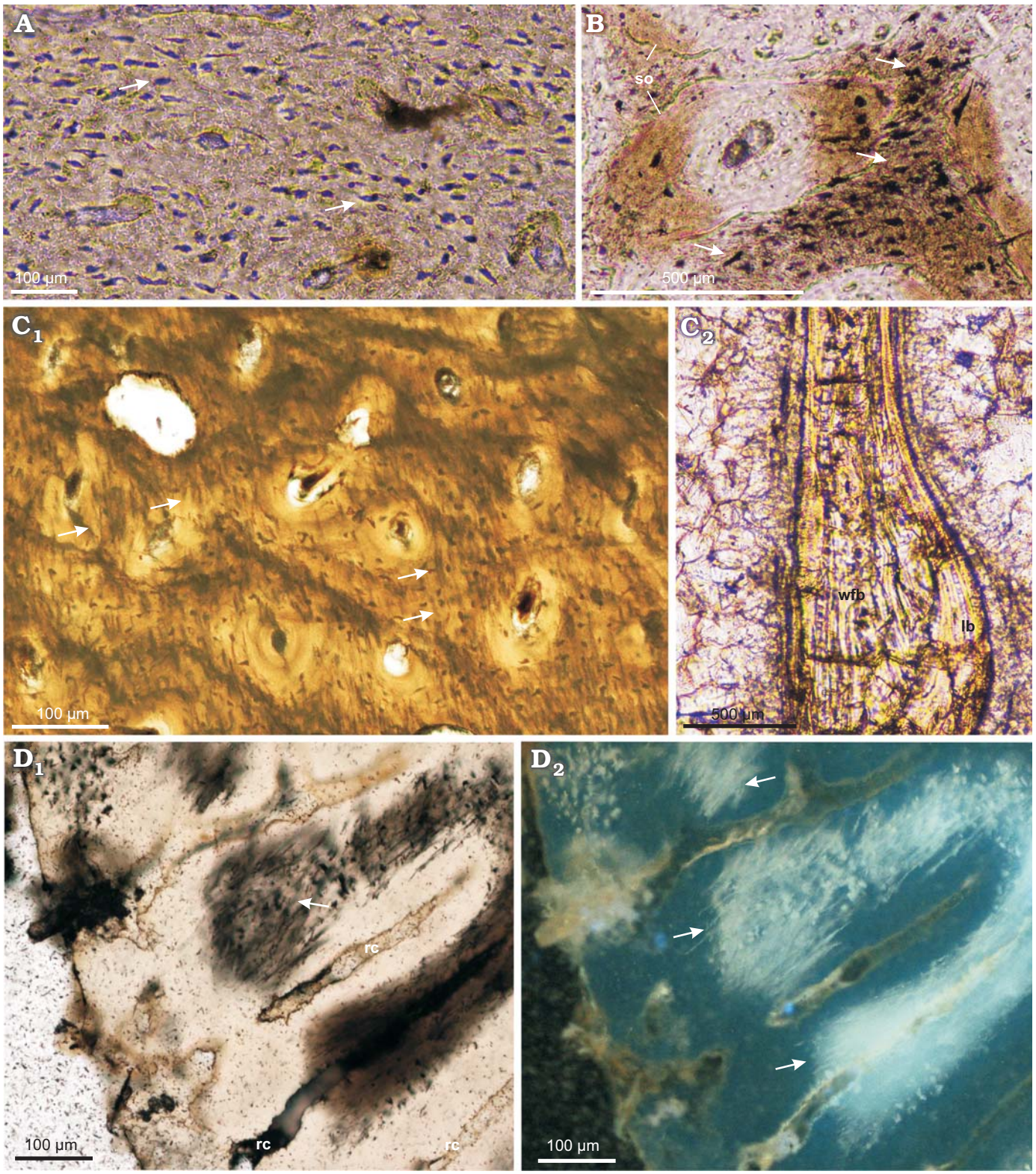

Fig. 3. Long bones microstructure of *Protoceratops andrewsi* Granger and Gregory, 1923, Toogreek (A) and Bayn Dzak (B–D), Mongolia, Late Cretaceous. **A**, **B**. Osteocyte lacunae (arrows) in cortex of subadult tibia ZPAL MgD-II/35c (**A**) and juvenile femur ZPAL MgD-II/407 (**B**). **C**. ZPAL MgD-II/11b, adult fibula showing in situ arrangement and abundance of fossilized fibers (arrows) in the cortex (C_1) and a structure of the trabeculae with woven-fibered bone in the core lined with lamellar bone (C_2). **D**. ZPAL MgD-II/3d, subadult femur with flocculated collagenous fibers (arrows) at the polished cross section. A–C, D_1, normal light; D_2, UV light. Abbreviations: lb, lamellar bone; rad, radial canals; so, secondary osteons; wfb, woven-fibered bone.

Rib.—The rib tissue has been studied only in ZPAL MgD-II/3b; thus, the data on the microstructure of this bone element should be treated as preliminary. The rib of *Protoceratops* is a strongly flattened and gently arched bone

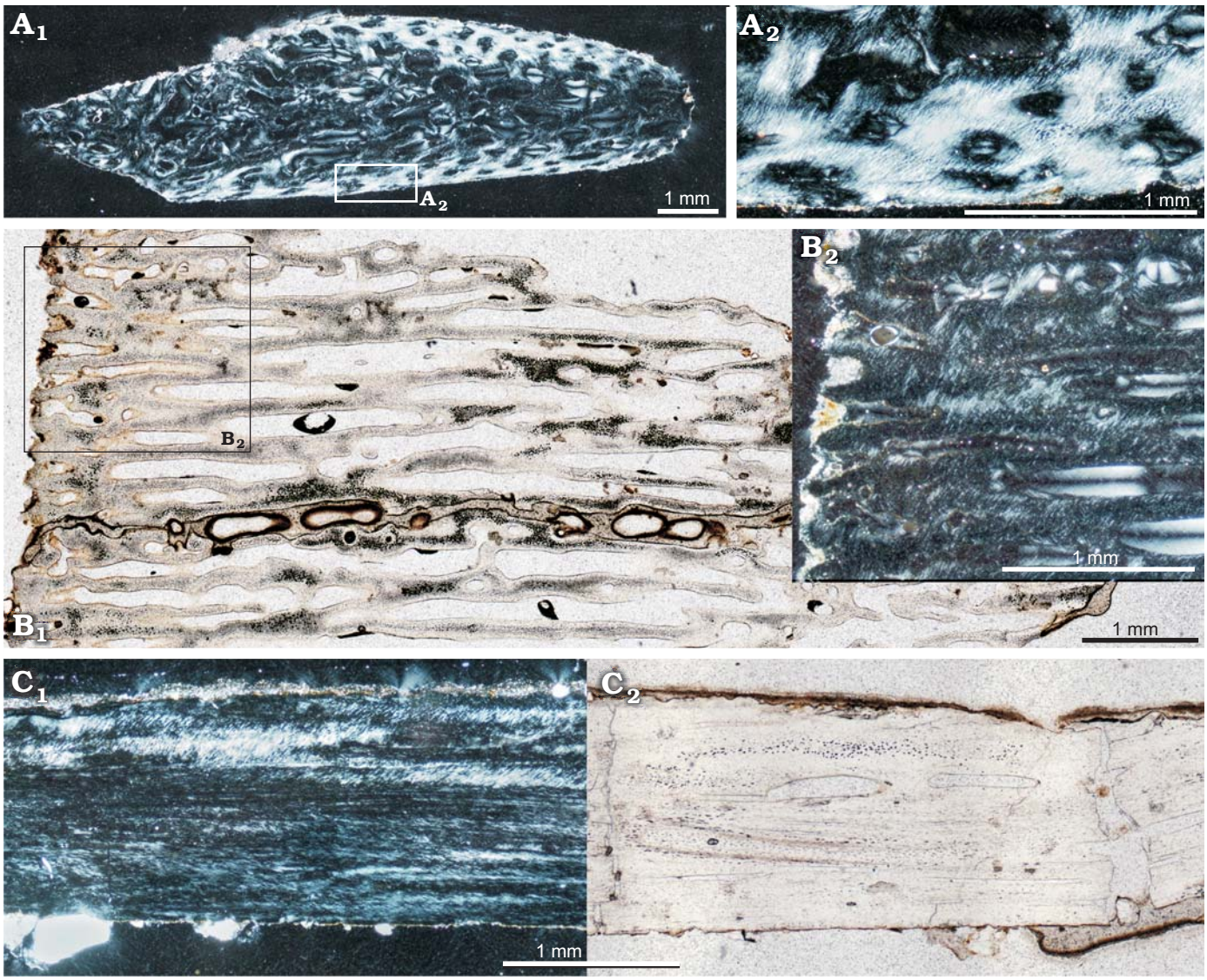

Fig. 4. Bone microstructure of parietal frill in subadult *Protoceratops andrewsi* Granger and Gregory, 1923, Bayn Dzak, Mongolia, Late Cretaceous (ZPAL MgD-II/3a). **A**. Sagittal section through the distal frill margin (A_2, magnification of the outer layer, magnified inset). **B**. Tangential section of the distal frill margin (B_2, magnified fragment). **C**. Sagittal section of frill plate; note the discrete zonation, compactness of the tissue, and acute angle fiber arrangement. B_1, C_2, normal light; A, B_2, C_1, polarized light.

showing a thick layer of primary bone tissue, which forms a thick external cortex (Fig. 6) and endosteal bone filling the center of the rib, sandwiched between the external layers. The bone matrix of the cortex shows dense fibers generally arranged parallel to the outer bone surface, but too unordered to form typical parallel-fibered bone (Fig. 6). There is a subtle "zonation" marked in the cortex portion, but no recognizable LAGs. Within the cortex, nascent and relatively rare small canals are formed, although without the surrounding lamellar bone of primary osteons yet. The canal diameter increases towards the core and in the deeper cortex some larger erosion lacunae are formed. The endosteal margin of the cortex is coarsely wavy showing the line of erosion of the cortex tissue. The internal part of the rib is filled with the compacted coarse cancellous bone formed endosteally. The tissue is densely packed and vacuities in this inner portion of the rib are minute, if present. No clearly delineated secondary osteons are present in the internal portion of the rib, but rather the entire space is filled with differently arranged layers of the lamellar tissue. On the other hand, the cortex bears no signs of secondary tissue and the remodeling manifests itself only in the erosion of cortex internal margin.

Long bones.—*Juveniles*: A juvenile femur ZPAL MgD-II/407 shows typical bone tissue dominated by the woven-fibered bone matrix (Fig. 2A), characteristic of young tetrapods (e.g., Chinsamy-Turan 2005; Curry 2008; Padian and Lamm 2013) with densely embedded, but still small primary osteons (Fig. 2). The osteons are nascent, displaying only a few layers of lamellar bone surrounding the canal. The matrix of the cortex shows small bundles of parallel arranged fibers,

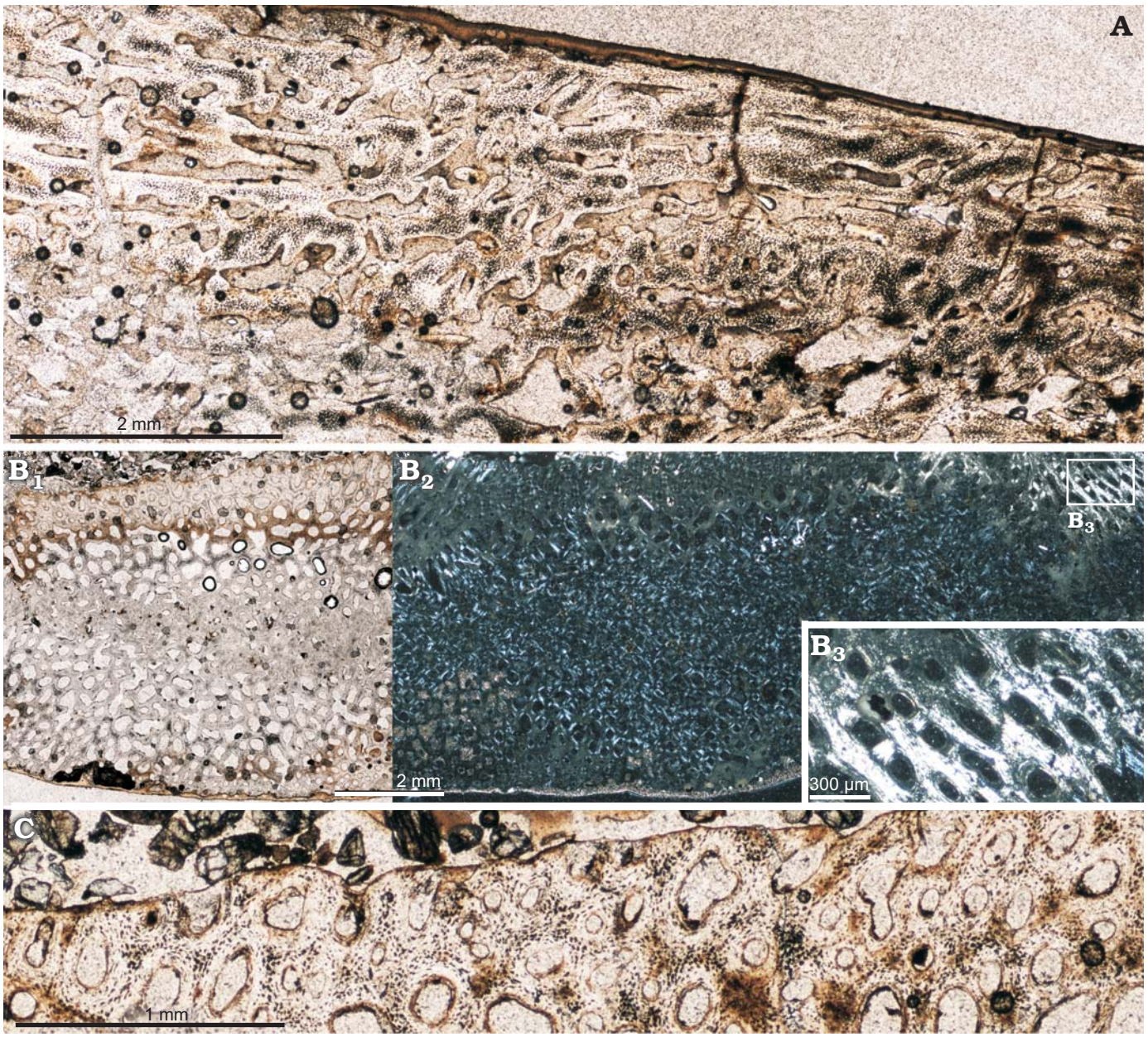

Fig. 5. Bone microstructure of the parietal frill in adult *Protoceratops andrewsi* Granger and Gregory, 1923, Bayn Dzak, Mongolia, Late Cretaceous (ZPAL MgD-II/33). **A**. Sagittal section. **B**, **C**. Transversal sections; note the condensations of the fossilized collagen fibers strengthening the porous tissue (**B**) and the formation of the small erosion lacunae at the external surface of the frill (**C**). A, B_1, C, normal light; B_2, B_3, polarized light.

which are especially well-visible in the outer part of the cortex (Fig. $2A_2$).

The marrow cavity sectioned in the mid-shaft of the femur is mostly empty, but its perimeter is lined with the coarse cancellous bone tissue and the remnants of trabeculae composed of the endosteal lamellar bone. The width of this band changes around the perimeter of the marrow cavity in a juvenile femur, most probably because the cutting was close to the base of the fourth trochanter. In the deeper cortex (and external medullar region, Fig. 7) some small secondary osteons can be observed, delineated clearly by cement lines (Fig. $7A_2$). They are, however, markedly separate and still embedded in the primary, woven-fibered bone matrix.

The tissue of a juvenile tibia ZPAL MgD-II/408, which is a larger (ca. 30% of an adult size) of two juvenile individuals studied by us, is very similar to that of the femur. Additionally, it shows a series of three to four wavy polishing lines in the cortex (Fig. $7B_2$, B_3). The polishing lines (see Sander 2000) are the fine growth lines more thin and delicate than the LAGs and seen only under some conditions on the surface of the bone sections. In some cases in our material the state of preservation of the bone matrix, which, during preparation became semi-translucent and opaque, enhanced visibility of the polishing lines, otherwise undetectable under the normal light.

The small tibia was sectioned more closely to the distal

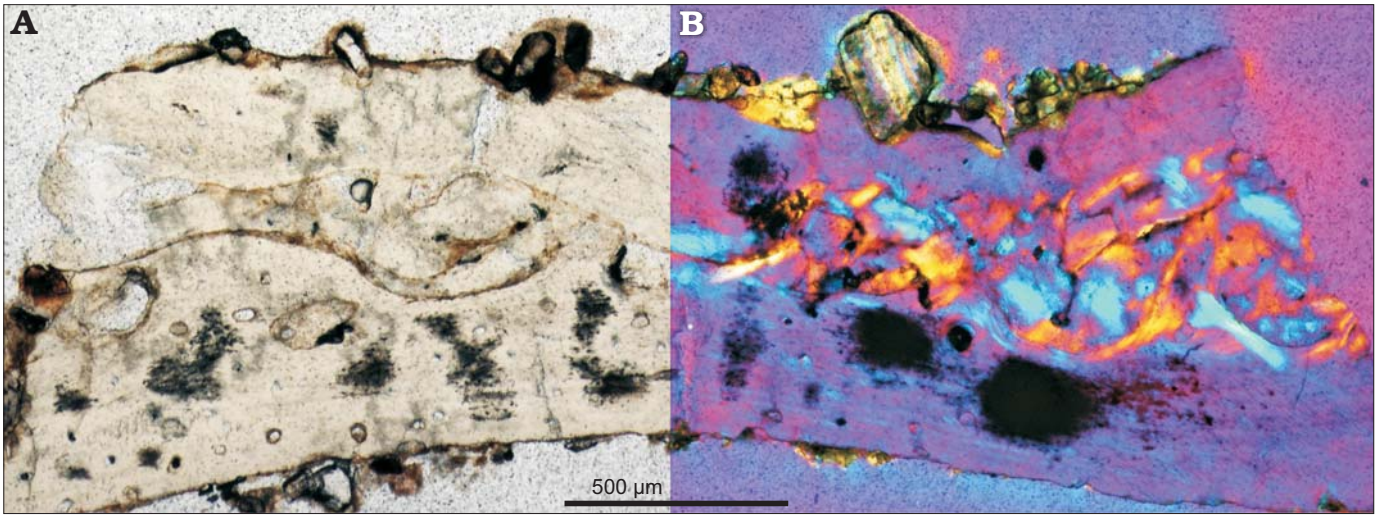

Fig. 6. Cross-section of the rib of *Protoceratops andrewsi* Granger and Gregory, 1923, Bayn Dzak, Mongolia, Late Cretaceous (ZPAL MgD-II/3); note the external cortex made of primary bone and extensively remodeled core formed by coarse cancellous bone tissue; in normal (**A**) and polarized (**B**) light.

epiphysis, thus the cortex is more porous (Fig. $7B_1$). Small erosion cavities appear already in its deeper part and become denser in the medullar region, which is mostly made of a dense spongiosa, still formed mostly in the primary woven-fibered bone with developing endosteal lining (Fig. $7B_1$).

The vascularization pattern of the juvenile long bones is prevailingly longitudinal and is maintained as such throughout the whole compacta (Figs. $2A_1$, $7A_1$, B). Also, density of the canals in the juvenile bone tissue is high, and uniform between the outer and inner cortex. In some regions of the cortex the canals with a radial or occasionally branching off arrangement can be recognized, implying a slight acceleration in growth during the bone deposition. A bone remodeling is rather low in both juvenile bones except in close vicinity of the perimedullar region where the endosteal bone appears (Fig. $7B_1$).

Subadults: Bone microstructure of subadult individuals is very similar to that of juveniles (Fig. 2); the differences mainly concern the arrangement of the bone fibers in the bone matrix. The cortex of the subadults shows some zonation, marked by the intercalating zones of concentrated parallel-fibered bone and woven-fibered tissue (Figs. $2B_2$, 8A, B_1, C_1, D). They are very well visible in the humerus (ZPAL MgD-II/3c, ZPAL MgD-II/15) and tibia (ZPAL MgD-II/35c), but very poorly developed in the femur (ZPAL MgD-II/35b), which overall has a very densely vascularized cortex composed in larger part of a woven-fibered bone tissue (Fig. 8C). The number of zones observed in the same individual (ZPAL MgD-II/35) varies among the humerus, femur, and tibia. In the humerus there are four distinct zones each ending with a distinct and wide band of a parallel-fibered bone (Fig. 8A). In the tibia the pattern is very similar but six to seven growth periods can be distinguished (Fig. 8E). On the other hand, the tissue of the femur shows only three poorly defined intercalating zones of less and more vascularized tissue (Fig. 8C). The less vascularized bands are dominated by the parallel-fibered bone matrix (Fig. $8C_2$), whereas more highly vascularized bone displays less arranged fibers in the bone matrix (woven-fibered type). The transitions between these zones show a change in the canal arrangement; the canals immediately adjacent to the parallel-fibered zone show a strong radial elongation, although they are not typical radial canals (Fig. $8C_1$, C_2). Another studied femur (ZPAL MgD-II/3d) does not exhibit any regular zonation but two bands of a dense parallel-fibered bone can be detected in its cortex, the one close to the bone circumference, and the second, ca. 80 µm thick, in a more internal layer (Fig. 8D). These condensation layers, too thick to be called annuli, change their width and intensity around the bone circumference. The tissue between the condensed layers of parallel-fibered bone shows typical woven-fibered bone matrix with multiple small primary osteons, implying that the bone deposition tempo was relatively quick, probably even quicker than that in the corresponding humerus.

The overall canal arrangement in the subadult bone tissue is prevailingly longitudinal with some local variation. In the humerus (ZPAL MgD-II/35a) the canals in the outer cortex are longitudinal but arranged in circular layers coaxial with the bone circumference (Fig. $8B_1$). In the tibia the canal arrangement is predominantly longitudinal in the outermost region of the cortex, then changes to mixed longitudinal-reticular, before finally changing to a somewhat laminar arrangement in the deep cortex.

The traces of remodeling are very limited in the subadult bones (Fig. 8A, B_2). The process manifests mostly in the humeral and tibial deep cortex in the form of lamellar filling of the erosion lacunae (Fig. 8A, B_2). On the other hand, the deeper cortex of femora formed of a typical fibro-lamellar tissue shows only eroded canals, enlarged to 20–100 µm in diameter, still mostly in the primary bone, with a nascent lamellar bone lining (Fig. $8E_2$).

Adults: Compared with the subadult bones, the compacta of the adult ulna (ZPAL MgD-II/8, Fig. 9A) and femur

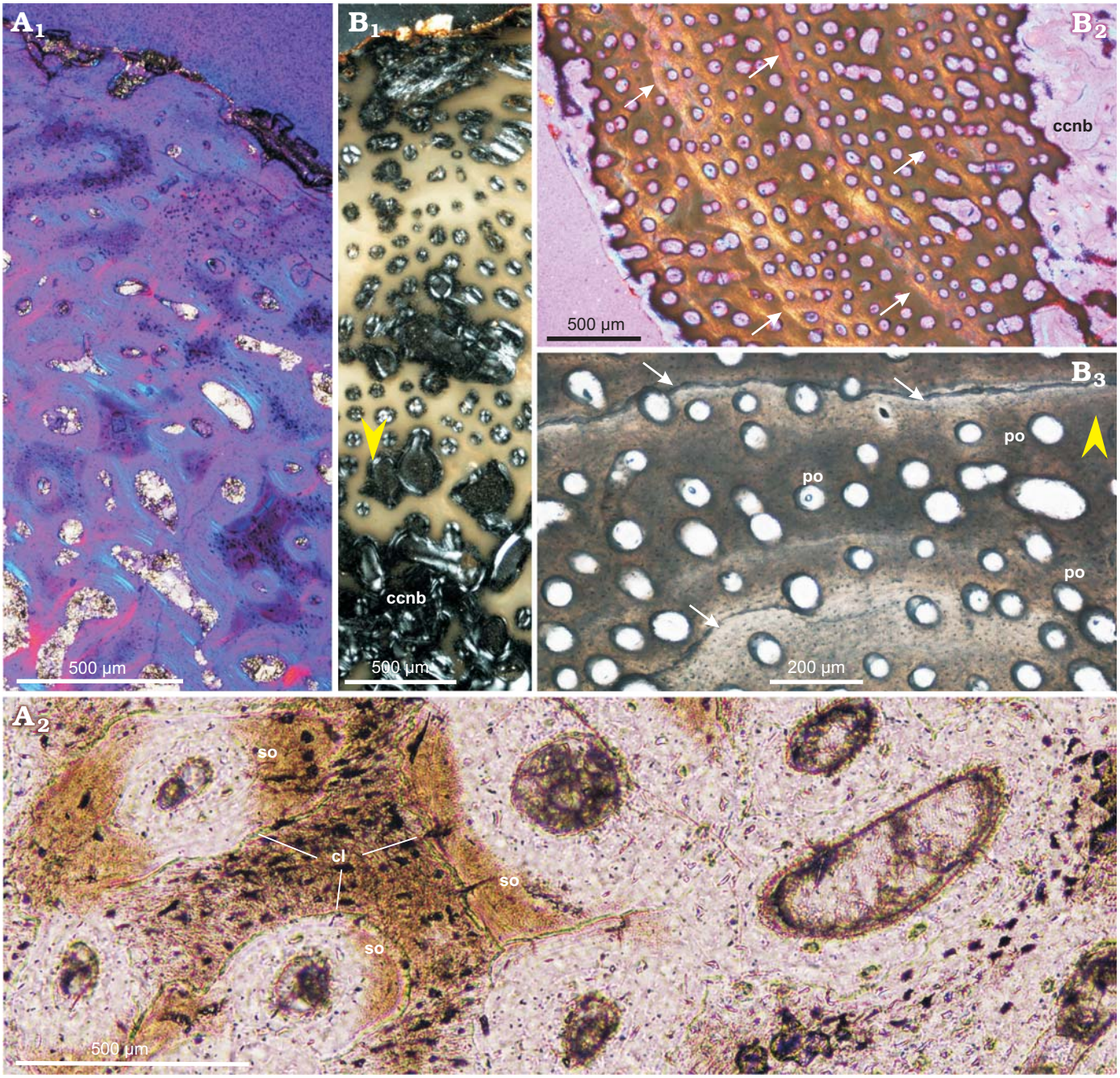

Fig. 7. Bone microstructure of juvenile femur (**A**) and tibia (**B**) of *Protoceratops andrewsi* Granger and Gregory, 1923, Bayn Dzak, Mongolia, Late Cretaceous. **A**. ZPAL MgD-II/407; outer cortex (A_1), showing small patches of parallel-fibered bone (light blue) and multiple primary osteons; canals are arranged longitudinally and the more internal cortex bears forming erosion lacunae; inner cortex (A_2). **B**. ZPAL MgD-II/408, section of the whole compacta showing coarse cancellous bone lined with endosteal lamellar bone in perimedullar region (B_1); tibial cortex displaying polishing lines indicated by arrows (B_2, B_3). Yellow arrowheads show outer bone perimeter. A_1, B, polarized light; A_2, normal light. Abbreviations: ccnb, coarse cancellous bone; cl, cement lines; po, primary osteons; so, secondary osteons.

(ZPAL MgD-II/11a, Fig. 9C) shows a better developed and more abundant parallel-fibered bone matrix. The parallel-fibered bone in the ulna is arranged in patches (Fig. 9A_1, A_2), but in the femur it forms irregularly spaced zones (most easily recognizable under polarized light, Fig. 9C_2), intercalated by the layers of woven-fibered bone. The mid-cortex, containing the bone deposited earlier in ontogeny (than that of the outer cortex), displays a less organized matrix with sub-checkered pattern of fiber orientation, especially in the femur. In the ulna the mid-cortex shows some signs of early stage remodeling; the diameter of the canals has increased and the layers of lamellar bone surrounding the osteons have thickened, forming a typical fibrolamellar complex (Fig. 9A_2, A_3). On the other hand, in the mid-cortex of the femur, instead of the wide zones of parallel-fibered bone a few annuli appear, separated by the wide zones of the

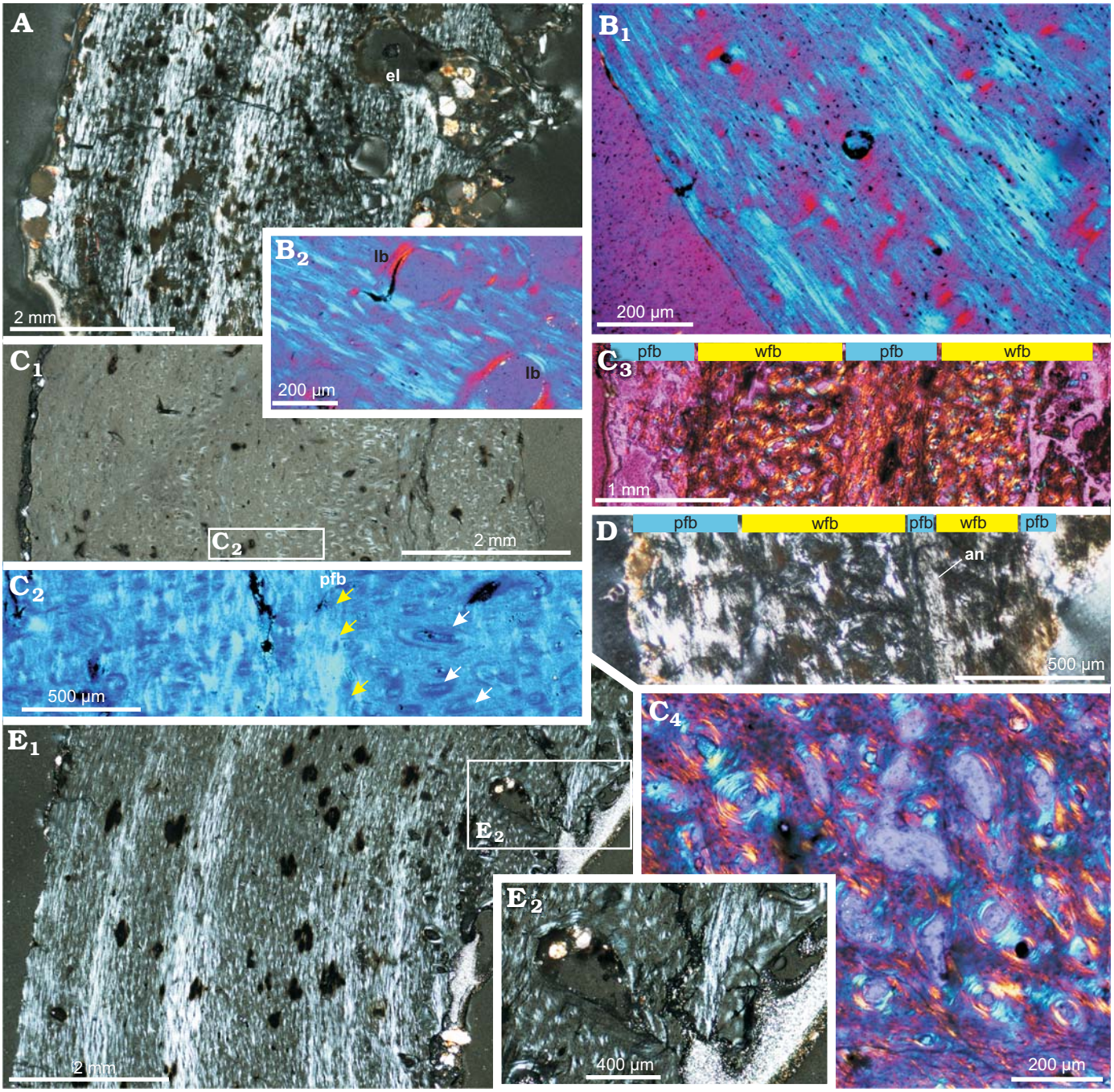

Fig. 8. Bone microstructure of subadult *Protoceratops andrewsi* Granger and Gregory, 1923, Toogreek (A, C, E) and Bayn Dzak (B, D), Mongolia, Late Cretaceous. **A**. Humerus ZPAL MgD-II/35a, total view of the compacta displaying patches of parallel-fibered bone (light bands) intercalated by zones of woven-fibered bone with multiple primary osteons (dark bands); note erosion lacunae in the inner cortex. **B**. Humerus ZPAL MgD-II/15, external cortex showing primary osteons and plies of the parallel fibered bone matrix (B_1), perimedullar region showing lamellar bone lining erosion lacunae in primary woven-fibered bone tissue (B_2). **C**, **D**. Compacta of femora. **C**. ZPAL MgD-II/35b, section showing modulations in canal arrangement and bone matrix; C_1, general picture of the whole bone wall; C_2, magnification illustrating thick band (yellow arrows) of the parallel-fibered bone and longitudinal canals changing orientation to radial (white arrows); C_3, section placed closer to the epiphysis, showing stronger zonation in bone matrix type; C_4, deep cortex showing enlarged canals in a woven-fibered bone. **D**. ZPAL MgD-II/3d, cortex showing ill defined annulus and less clear modulations of the bone matrix. **E**. Tibia ZPAL MgD-II/35c, whole compacta (E_1) and deep cortex (E_2). The section displays a typical fibrolamellar bone complex with zonation in the bone matrix. The outer cortex displays zones of parallel-fibered bone matrix intercalated with the zones of more chaotically oriented collagen fibers, the perimedullar region shows larger erosion lacunae filled with endosteally formed lamellar bone (E_2). A, C_1, D, E, polarized light; B, C_2–C_4, polarized light (quartz wedge). Abbreviations: an, annulus; el, erosion lacunae; lb, lamellar bone; pfb, parallel-fibered bone; wfb, woven-fibered bone.

woven-fibered bone (Fig. 9C_1, C_3). In total, about seven growth marks (mostly better or worse defined annuli) can be distinguished in the adult femur, while they are not visible in the ulna.

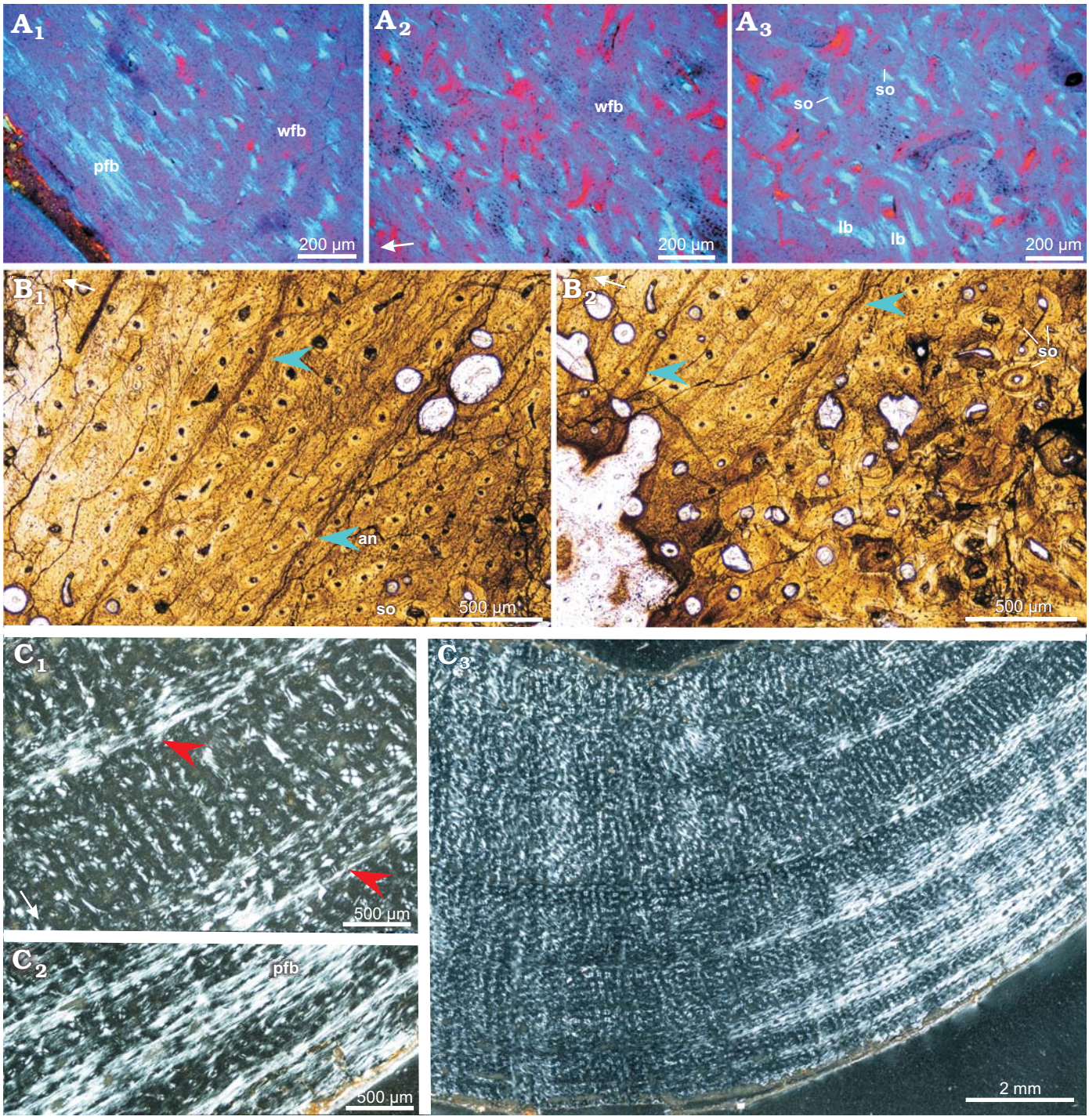

Fig. 9. Bone microstructure in adult *Protoceratops andrewsi* Granger and Gregory, 1923, Bayn Dzak, Mongolia, Late Cretaceous. **A**. Ulna ZPAL MgD-II/8, matrix in the outer (A_1) and mid-cortex (A_2), perimedullar region with endosteally-formed lamellar bone (A_3). **B**. Fibula ZPAL MgD-II/11b; note well formed LAGs (blue arrowheads) and annulus in the cortex (B_1); deeper cortex shows signs of remodeling and multiple secondary osteons (B_2). **C**. Femur ZPAL MgD-II/11a, compacta showing wider zones of fast growing woven-fibered bone intersected by thin annuli of parallel-fibered bone (red arrowheads) in the mid-cortex (C_1, C_3); condensation of the parallel-fibered bone zones in the outer cortex (C_2). A, polarized light (quartz wedge); B, normal light; C, polarized light. White arrows point outward. Abbreviations: an, annulus; lb, lamellar bone; pfb, parallel-fibered bone; so, secondary osteons; wfb, woven-fibered.

Throughout most of the cortex (apart from the most internal regions) of the adult bones, the canal arrangement and orientation are mostly longitudinal (Fig. 9), although some canals are oriented differently. In the outer cortex of the adult femur the longitudinal canals are arranged in a laminar pattern, while the deep cortex shows a mix of longitudinal and radial canals. In the ulna and fibula, longitudinal canal pattern is maintained throughout the whole cortex. The density of the primary osteons is high, although slightly reduced in the outermost regions of the cortex.

In adult bones, the extent of the porosity in the cortex is similar to that of the subadult bones and starting with the more internal parts of the cortex it increases slowly towards the medullar cavity. In adult humerus and ulna larger erosion lacunae are nested in the deeper regions of the cortex and lined with the lamellar bone of endosteal origin. Although the sectioned adult femora usually show weakest remodeling and lack secondary osteons entirely, in ZPAL MgD-II/16b multiple erosion lacunae of small diameter (25–50 μm) are scattered across the deeper regions of the compacta, while the larger lacunae, located in the perimedullary region, are lined with lamellar bone. In an adult ulna the porosity of the deep cortex increased (in comparison with that of the femur) and typical cancellous bone lined with the endosteal lamellar tissue has begun to form. The entire perimedullar region of the ulna is much more extensively remodeled (Fig. $9A_3$), although rare patches of primary tissue, packed densely with osteocyte lacunae, still can be distinguished (Fig. $9A_2$).

Among all the adult bones included in this study, the fibula ZPAL MgD-II/11b shows the highest degree of remodeling and largest amount of secondary bone tissue, although the level of remodeling is still only moderate compared with what has been reported in some other dinosaur genera (e.g., Horner et al. 2000; Chinsamy-Turan 2005). The fibula ZPAL MgD-II/11b is also the only adult bone that displays typical LAGs in the cortex (Fig. 9B). Four to five LAGs or narrow annuli can be distinguished in the non-remodeled part of the fibular cortex, although any other growth marks that once existed have been erased by the secondary bone tissue and bone drift. The perimedullar region comprises of dense coarse-cancellous bone rich in the endosteal lamellar deposits, which line the erosion lacunae and bone trabeculae, whose central portions still include woven-fibered primary tissue (Fig. $3C_2$).

Discussion

General remarks on the bone microstructure and growth pattern.—The long bone microstructure of *Protoceratops andrewsi*, which was a relatively small-size dinosaur, not exceeding 2 m in length (You and Dodson 2004: fig. 22.2C), is roughly similar to that of other "small dinosaurs", namely *Orodromeus*, *Psittacosaurus*, or *Scutellosaurus* (Padian et al. 2004). The prevailing longitudinal vascularization pattern and the bone matrix comprised mostly of the intermixed woven-fibered to parallel-fibered types (in different proportions regarding the age classes), indicate a moderate growth tempo. The growth was apparently slower than in large representatives of both Ornithischia (*Maiasaura*), and Saurischia (such as *Apatosaurus* or *Allosaurus*) (Horner et al. 2000; Padian et al. 2004; Curry 2008; Woodward et al. 2015). Among other small dinosaurs, the tempo of growth of *Protoceratops* is comparable to that of *Psittacosaurus* (Zhao et al. 2013) and the stem stegosaurid *Kentrosaurus* (Redelstorff et al. 2013), although in *Protoceratops* the bone tissue shows a slightly sparser vascularization than in any of the mentioned genera.

Most of the studied bone elements, apart from an adult fibula (Fig. 9B), do not display clear LAGs or well defined annuli, although the tissue is undoubtedly zonal, showing alternating zones of quickly and slowly accreted bone, characterized by changes in the bone matrix. Similar tissue zonation were observed also in *Leonerasaurus taquetrensis* (Cerda et al. 2017: fig. 10H), a diaphyseal section of the tibia in *Gasparinisaura cincosaltensis* (Cerda and Chinsamy 2012) or polar *Edmontosaurus*, although in the last case, the zones represented actually modulations of bone vascularization pattern, which varied between reticular and circumferential (Chinsamy et al. 2012).

The general opinion is that growth marks, especially LAGs, are an annual or at least strongly seasonal feature (e.g., Erickson and Tumanova 2000; Chinsamy-Turan 2005; Zhao et al. 2013). In the case of *Protoceratops*, the structure of the zones, showing transition from quickly to slowly accreted bone, may indicate a period of changing environmental conditions (perhaps with two regular seasons). Given the semi-desert paleoenvironment of the Djadokhta Formation (Osmólska 1980; Jerzykiewicz and Russell 1991; Jerzykiewicz et al. 1993), the most obvious factor might be water availability, decreasing with the end of the rainy season. Thus, a zone may have started as a quickly accreting tissue deposited under favorable conditions and then the tissue becomes more and more parallel-fibered until it forms a thick poorly defined annulus of a dense parallel-fibered tissue (which might be the record of the peak of the dry season); then a new cycle begins starting with the woven-fibered bone (Fig. 8A, C, E). The described pattern is well expressed in the humerus and tibia, while in the femur (especially in juveniles and subadults) the modulations are much subtler (mostly seen as a slight change in the canal orientation, showing some radial deviation, Fig. $8C_1$). The changes in canal arrangement resemble more closely those found in *Edmontosaurus*, interpreted as the record of the polar day and night intervals (Chinsamy et al. 2012). Regardless of the exact cause, we can suppose that a full depositional cycle from the quickly accreting tissue to most condensed band of parallel-fibered bone represents the seasonal cycle, approximately of one year duration. Taking this into account, we can assume that the smallest individuals, which exhibit three to five zones, of which the innermost is preserved only fragmentary because of the bone drift (see Chinsamy-Turan 2005), would have been approximately 3–5 years old at the moment of death, and therefore comparable to the growth stages A to B of *Psittacosaurus mongoliensis* (see Erickson and Tumanova 2000).

When the juvenile, subadult, and adult bone tissue of the fore- and hindlimbs of *Protoceratops* are compared, they show slightly differing growth patterns. Juvenile bones show poorly expressed zonation (marked only by polishing lines) or no zonation at all, and these zones are usually

equally thick. In subadults and adults the mid-cortex zones are usually the thickest. Furthermore, comparisons between the growth pattern of the humerus, femur, and tibia in the same subadult individual (ZPAL MgD-II/35) expressed in the thickness and tissue morphology, show that in the humerus and tibia the bone accretion was similar but in the femur the parallel-fibered bone matrix was much scarcer, favoring formation of woven-fibered bone, which implies faster bone formation. Growth of the femur slows down after the fifth depositional cycle (recognizable at the bone section), and the zones formed by woven-fibered bone become increasingly narrow, while those formed by parallel-fibered bone thicken until they dominate most of the matrix.

Attaining of sexual (but not full somatic) maturity was proposed as an explanation for similar changes (i.e., shift in the character of the bone matrix and a slower deposition rate) in other ornithischians (e.g., Redelstorff et al. 2013). We concur with this interpretation; thus it follows that the femur was the most rapidly growing bone in subadult *Protoceratops* and that its growth started to slow probably when the animal neared sexual maturity. The bones of the fore- and hindlimbs of adult specimens show a smaller disparity in the content of parallel fibered bone matrix, in the external cortex, although an adult femur still displays the least extent of this type of the bone (Fig. $9C_3$).

The density of vascularization and canal orientation in the external cortex of an adult forelimb (i.e., ulna) and hindlimbs (i.e., femur) are almost the same. Both indicate some decrease in the rate of the bone deposition, but suggest that bone tissue was still being deposited even in a fully grown animal.

Patterns of limb bone growth in *Protoceratops* and *Psittacosaurus* show some similarities, although the growth tempo in *Protoceratops* seems slower than that of *Psittacosaurus* (Zhao et al. 2013), judging on the basis of higher content of parallel-fibered bone and sparser canals with the prevailingly longitudinal, poorly anastomosing arrangement in the former. In *Psittacosaurus* the humeral growth rate was highest between the second and third year, and for the femur between the third and sixth year (Zhao et al. 2013). Changes in bone tissue during ontogeny in *Psittacosaurus* were explained by a shift from quadrupedal to bipedal mode of locomotion (Erickson and Tumanova 2000; Zhao et al. 2013). There is a general agreement that adult *Protoceratops* was quadrupedal (Dodson et al. 2004; Lee et al. 2011), as its body and head were too heavy for bipedal locomotion. Nevertheless, the peak observed in the rate of the femoral bone deposition at early subadult stage of *Protoceratops* and also changes in the limb bone proportions (JS unpublished data) suggest the relatively quicker growth of the hind limb bones, which point to a possibility of facultative bipedality of young *Protoceratops*. Further comprehensive studies of ontogenetic changes in the skeleton of *Protoceratops* would be needed to reconstruct its range of locomotor adaptations and their implications for *Protoceratops* lifestyle.

Bone fibers.—One of the noticeable features of *Protoceratops* bone tissue is a high content of fossilized fibers, observed not only in the parietal frill tissue, similar to that reported for *Triceratops* (Horner and Lamm 2011), but also in the long bone tissue. The fiber density in the frill tissue was explained as an adaptive character towards strengthening the frill structure in *Triceratops* and facilitating the adhesion of the soft tissue covering the frill (Horner and Lamm 2011).

The structure of the parietal frill in *Protoceratops andrewsi* is similar to that observed in the frill of *Triceratops* (Horner and Lamm 2011), especially in the case of subadult individuals. The frill in both taxa is a bony structure covered by a thick skin, although it was much more expanded (and thus, heavier) in *Triceratops* than in *Protoceratops*. Consequently, load of strain acting on the bone of the frill in *Protoceratops* was apparently much lower than that in *Triceratops*. This factor resulted in the lack of extensive tissue hyperostosis in the former even in the largest of the studied individuals, the feature otherwise observed in mature *Triceratops* (Horner and Lamm 2011). Also, the frill microstructure in *Protoceratops* does not show any signs of the extensive resorption or tissue metaplasia even in large specimens. However, it is also highly porous and expresses a large density of Sharpey's fibers. The abundance of Sharpey's fibers is typical of bone elements prone to mechanical stress (see the scapula of *Kentrosaurus*; Redelstorff et al. 2013: fig. 9), either from muscle or tendon attachments or covered immediately by skin or keratin sheath (a horn or beak). Apart from the bone frill of *Triceratops*, such fiber concentration was also observed in the bones of the snout region in dicynodonts, well known to bear a keratin beak (Jasinoski and Chinsamy-Turan 2012).

High fiber content observed by us not only in the tissue of the frill but also in the limb bones of *Protoceratops* (noticeable also in *Psittacosaurus*, see Zhao et al. 2013: fig. S1c) implies that the feature might have been characteristic of the ceratopsian bone and as such might have turned out a prerequisite for the expansion of the parietal bone forming the frill.

Bone remodeling.—As far as the bone remodeling of *Protoceratops* is concerned, the juvenile bone tissue displays only an incipient remodeling, similar to that in *Psittacosaurus*. This process is best expressed in an adult fibula but it is still very weak compared with the completely remodeled bones with overlapping secondary osteons, found in other ornithischians, e.g., saurolophs (Horner et al. 2000). The interpretation of the extent of remodeling is still a disputed issue in vertebrate paleohistology (Chinsamy-Turan 2005 and references therein; Padian and Stein 2013). According to the currently prevailing opinion, a high remodeling ratio does not necessarily implies higher metabolic rates (Chinsamy-Turan 2005), as it is usually relatively low in endotherms (e.g., Chinsamy 1997, 2002; Chinsamy and Elzanowski 2001; Starck and Chinsamy 2002; Padian et al. 2004). Instead, it may be related to the mechanical stress, caused either by the size of an animal or its mode of locomo-

tion as it was presumed in the case of *Syntarsus* (Chinsamy 1990; Chinsamy-Turan 2005). However, the strict correlation between the intensity of mechanical stress and extent of remodeling was questioned by Horner et al. (1999).

In the case of *Protoceratops*, its metabolic ratio was most probably relatively low, due to a herbivorous diet and small size meant that a low stress applied to the skeletal elements of this animal, which both may have contributed to a low content of secondary bone. The latter factor seems quite well supported for *Protoceratops*, which was generally compact and apparently slow-moving, quadrupedal dinosaur, with only a moderately heavy head (with a medium-sized frill).

The tissue of the femur and tibia in the largest studied by us individual of *Protoceratops andrewsi* (ZPAL MgD-II/11a, c) does not show any External Fundamental System (EFS) of the kind found in some large dinosaurs (Horner et al. 2000), pterosaurs (Padian et al. 2004), or even (although poorly expressed) in dinosauromorphs (Fostowicz-Frelik and Sulej 2010). In particular, the most external cortex still shows some vascularization and there is no trace of true lamellar bone at the bone outermost layers, which are still formed by parallel-fibered bone only. This suggests that after animal's somatic maturity the growth slowed visibly, although its basic rate was close to that of *Psittacosaurus* (Erickson and Tumanova 2000; Zhao et al. 2013). In contrast to our findings, Makovicky et al. (2007) reported formation of EFS in *Protoceratops*, although they stated that the extent of EFS and its exact structure is strongly intra-specifically variable in the sample studied by them. To address this discrepancy, a more abundant sample of the oldest individuals of *Protoceratops* has to be studied.

Conclusions

The bone tissue microstructure of *Protoceratops andrewsi* is similar to that of other small herbivorous dinosaurs such as *Psittacosaurus* or *Scutellosaurus*. A certain variability of tissue histology observed between different age stages is due to changing content of the parallel-fibered bone matrix, which increases with age. The bone matrix in the long bones is zonal, showing transition from the woven-fibered to parallel-fibered matrix with poorly expressed annuli. This may reflect seasonality and varying water availability in the semi-desert environs of the Djadokhta Formation (Late Cretaceous, Mongolia). The parietal frill microstructure is similar to that of *Triceratops* but shows virtually no hyperostosis, smaller erosion cavities, and overall a more juvenile morphology, while lacking any metaplastic traits, even in mature individuals. The remodeling is very limited at all age stages. We did not observe the EFS formation even in adults. This suggests that *Protoceratops* grew throughout most of its life (at least until advanced mature age). Further studies on larger samples of various ontogenetic age are needed to estimate its growth tempo and the stage when growth of *Protoceratops* terminated (specifically, if EFS was present).

Acknowledgements

We thank Zbigniew Strąk and Adam Zaremba (ZPAL) for preparing the thin-section slides; we are grateful also to Krzysztof Owocki (ZPAL) for allowing us to study some of the thin-section slides prepared by him; Jarosław Stolarski and Katarzyna Frankowiak (both ZPAL) are cordially thanked for the access to a fluorescence microscope. Thanks are also extended to Michał Surowski (Department of Geology, University of Warsaw, Poland) for the access and help with a polarizing microscope Nikon Eclipse LV100 POL. We are extremely grateful to Ignacio A. Cerda (Consejo Nacional de Investigaciones Científicas y Técnicas, Universidad Nacional de Rio Negro, Argentina) and Anusuya Chinsamy-Turan (University of Cape Town, South Africa) for helpful comments on the manuscript.

References

Brown, B. and Schlaikjer, E.M. 1940. The structure and relationships of *Protoceratops*. *Annals of the New York Academy of Sciences* 40: 133–266.

Cerda, I.A. and Chinsamy, A. 2012. Biological implications of the bone microstructure of the Late Cretaceous ornithopod dinosaur *Gasparinisaura cincosaltensis*. *Journal of Vertebrate Paleontology* 32: 355–368.

Cerda, I.A., Chinsamy, A., Pol, D., Apaldetti, C., Otero, A., Powell, J.E., and Nestor Martinez, R. 2017. Novel insight into the origin of the growth dynamics of sauropod dinosaurs. *PLoS ONE* 12 (6): e0179707.

Chinsamy, A. 1990. Physiological implications of the bone histology of *Syntarsus rhodesiensis* (Saurischia: Theropoda). *Palaeontologia Africana* 27: 77–82.

Chinsamy, A. 1997. Assessing the biology of fossil vertebrates through bone histology. *Palaeontologia Africana* 33: 29–35.

Chinsamy, A. 2002. Bone microstructure of early birds. *In*: L.M. Chiappe and L.M. Witmer (eds.), *Mesozoic Birds*: *Above the Heads of Dinosaurs*, 421–431. University of California Press, Berkeley.

Chinsamy, A. and Elzanowski, A. 2001. Evolution of growth pattern in birds. *Nature* 412: 402–403.

Chinsamy, A., Thomas, D.B., Tumarkin-Deratzian, A.R., and Fiorillo, A.R. 2012. Hadrosaurs were perennial polar residents. *The Anatomical Record* 295: 610–614.

Chinsamy-Turan, A. 2005. *The Microstructure of Dinosaur Bone*. 216 pp. The Johns Hopkins University Press, Baltimore.

Curry, K.A. 2008. Ontogenetic histology of *Apatosaurus* (Dinosauria: Sauropoda): New insights on growth rates and longevity. *Journal of Vertebrate Paleontology* 19: 654–665.

Dodson, P. 1976. Quantitative aspects of relative growth and sexual dimorphism in *Protoceratops*. *Journal of Paleontology* 50: 929–940.

Dodson, P., Forster, C.A., and Sampson, S.D. 2004. Ceratopsidae. *In*: D.B. Weishampel, P. Dodson, and H. Osmólska (eds.), *The Dinosauria. Second Edition*, 494–516. University of California Press, Berkeley.

Erickson, G.M. and Tumanova, T.A. 2000. Growth curve of *Psittacosaurus mongoliensis* Osborn (Ceratopsia: Psittacosauridae) inferred from long bone histology. *Zoological Journal of the Linnean Society* 130: 551–566.

Erickson, G.M., Zelenitsky, D.K., Kay, D.I., and Norell, M.A. 2017. Dinosaur incubation periods directly determined from growth-line counts in embryonic teeth show reptilian-grade development. *Proceedings of the National Academy of Sciences of the United States of America* 114: 540–545.

Farlow, J.O. and Dodson, P. 1975. The behavioral significance of frill and horn morphology in ceratopsian dinosaurus. *Evolution* 29: 353–61.

Fastovsky, D.E., Badamgarav, D., Ishimoto, H., Watabe, M., and Weishampel, D.B. 1997. The paleoenvironments of Tugrikin-Shireh (Gobi Desert, Mongolia) and aspects of the taphonomy and paleoecology of *Protoceratops* (Dinosauria: Ornithischia). *Palaios* 12: 59–70.

Fastovsky, D.E., Weishampel, D.B., Watabe, M., Barsbold, R., Tsogtbaatar, K., and Narmandakh, P. 2011. A nest of *Protoceratops andrewsi* (Dinosauria, Ornithischia). *Journal of Paleontology* 85: 1035–1041.

Fostowicz-Frelik, Ł. and Sulej, T. 2010. Bone histology of *Silesaurus opolensis* Dzik, 2003, from the Late Triassic of Poland. *Lethaia* 43: 137–148.

Granger, W. and Gregory, W.K. 1923. *Protoceratops andrewsi*, a pre-ceratopsian dinosaur from Mongolia. *American Museum Novitates* 72: 1–9.

Hall, B.K. 2005. *Bones and Cartilage*: *Developmental and Evolutionary Skeletal Biology*. 760 pp. Elsevier Academic Press, Amsterdam.

Handa, N., Watabe, M., and Tsogtbaatar, K. 2012. New specimens of *Protoceratops* (Dinosauria: Neoceratopsia) from the Upper Cretaceous in Udyn Sayr, Southern Gobi Area, Mongolia. *Paleontological Research* 16: 179–98.

Hone, D.W.E., Farke, A.A., Watabe, M., Shigeru, S., and Tsogtbaatar, K. 2014. A new mass mortality of juvenile *Protoceratops* and size-segregated aggregation behaviour in juvenile non-avian dinosaurs. *PLoS ONE* 9: e113306.

Hone, D.W.E., Farke, A.A., and Wedel, M.J. 2016. Ontogeny and the fossil record: what, if anything, is an adult dinosaur? *Biology Letters* 12 (2): 20150947.

Horner, J.R. and Lamm, E.-T. 2011. Ontogeny of the parietal frill of *Triceratops*: A preliminary histological analysis. *Comptes Rendus Palevol* 10: 439–452.

Horner, J.R., Ricqlès, A. de, and Padian, K. 1999. Variation in dinosaur skeletochronology indicators: Implications for age assessment and physiology. *Paleobiology* 25: 295–304.

Horner, J.R., Ricqlès, A. de, and Padian, K. 2000. Long bone histology of the hadrosaurid dinosaur *Maiasaura peeblesorum*: Growth dynamics and physiology based on an ontogenetic series of skeletal elements. *Journal of Vertebrate Paleontology* 20: 115–29.

Jasinoski, S.C. and Chinsamy-Turan, A. 2012. Biological Inferences of the Cranial Microstructure of the Dicynodonts *Oudenodon* and *Lystrosaurus*. *In*: A. Chinsamy-Turan (ed.), *Forerunners of Mammals. Radiation, Histology, Biology*, 148–176. Indiana University Press, Bloomington.

Jerzykiewicz, T., Currie, P.J., Eberth, D.A., Johnston, P.A., Koster, E.H., and Zheng, J.-J. 1993. Djadokhta Formation correlative strata in Chinese Inner Mongolia: an overview of the stratigraphy, sedimentary geology, and paleontology and comparisons with the type locality in the pre-Altai Gobi. *Canadian Journal of Earth Sciences* 30: 2180–2190.

Jerzykiewicz, T. and Russell, D.A. 1991. Late Mesozoic stratigraphy and vertebrates of the Gobi Basin. *Cretaceous Research* 12: 345–77.

Lee, Y.N., Ryan, M.J., and Kobayashi, Y. 2011. The first ceratopsian dinosaur from South Korea. *Naturwissenschaften* 98: 39–49.

Maidment, S.C.R. and Barrett, P.M. 2014. Osteological correlates for quadrupedality in ornithischian dinosaurs. *Acta Palaeontologica Polonica* 59: 53–70.

Maiorino, L., Farke, A., Kotsakis, T., and Piras, P. 2015. Males resemble females: re-evaluating sexual dimorphism in *Protoceratops andrewsi* (Neoceratopsia, Protoceratopsidae). *PLoS ONE* 10: e0126464.

Makovicky, P., Sadleir, R., Dodson, P., Erickson, G., and Norell, M. 2007. Life history of *Protoceratops andrewsi* from Bayn Zag, Mongolia. *Journal of Vertebrate Paleontology* 27 (Supplement to No. 3): 109A.

Niedźwiedzki, G., Singer, T., Gierliński, G.D., and Lockley, M.G. 2012. A protoceratopsid skeleton with an associated track from the Upper Cretaceous of Mongolia. *Cretaceous Research* 33: 7–10.

Osmólska, H. 1980. The Late Cretaceous vertebrate assemblages of the Gobi Desert, Mongolia. *Mémoires Société Géologique de France* 139: 145–150.

Padian, K. and Lamm, E.-T. (eds.) 2013. *Bone Histology of Fossil Tetrapods*: *Advancing Methods*, *Analysis and Interpretation*. 285 pp. University of California Press, Berkeley.

Padian, K. and Stein, K. 2013. Evolution of growth rates and their implications. *In*: K. Padian and E.-T. Lamm (eds.), *Bone Histology of Fossil Tetrapods*, 253–264. University of California Press, Berkeley.

Padian, K., Horner, J.R., and Ricqles, A. de 2004. Growth in small dinosaurs and pterosaurs: the evolution of archosaurian growth strategies. *Journal of Vertebrate Paleontology* 24: 555–571.

Redelstorff, R., Hübner, T., Chinsamy, A., and Sander, M. 2013. Bone histology of the stegosaur *Kentrosaurus aethiopicus* (Ornithischia: Thyreophora) from the Upper Jurassic of Tanzania. *The Anatomical Record* 296: 933–952.

Sander, P.M. 2000. Longbone histology of the Tendaguru sauropods: implications for growth and biology. *Paleobiology* 26: 466–488.

Senter, P. 2007. Analysis of forelimb function in basal ceratopsians. *Journal of Zoology* 273: 305–314.

Starck, J.M. and Chinsamy, A. 2002. Bone microstructure and developmental plasticity in birds and other dinosaurs. *Journal of Morphology* 254: 232–246.

Tereshchenko, V.S. 1994. On the reconstruction of the static pose in *Protoceratops*. *Paleontological Journal* 28: 85–97.

Tereshchenko, V.S. 1996. A reconstruction of the locomotion of *Protoceratops*. *Paleontological Journal* 30: 232–245.

Woodward, H.N., Freedman Fowler, E.A., Farlow, J.O., and Horner, J.R. 2015. *Maiasaura*, a model organism for extinct vertebrate population biology: A large sample statistical assessment of growth dynamics and survivorship. *Paleobiology* 41: 503–527.

You, H. and Dodson, P. 2004. Basal Ceratopsia. *In*: D.B. Weishampel, P. Dodson, and H. Osmólska (eds.), *The Dinosauria. Second Edition*, 478–493. University of California Press, Berkeley.

Zhao, Q., Benton, M.J., Sullivan, C., Sander, M., and Xu, X. 2013. Histology and postural change during the growth of the ceratopsian dinosaur *Psittacosaurus lujiatunensis*. *Nature Communications* 4: 2079.

Zhou, C.F., Gao, K.Q., and Fox, R.C. 2010. Morphology and histology of lattice-like ossified epaxial tendons in *Psittacosaurus* (Dinosauria: Ceratopsia). *Acta Geologica Sinica* (*English Edition*) 84: 463–471.